Research Article

Aulia Windyandari, Ojo Kurdi*, Sulardjaka, and Mohammad Tauviqirrahman

Bow structure damage analysis for hybrid coir-glass fiber composite fishing boat hull subjected to front collision load

https://doi.org/10.1515/cls-2022-0020
Received Jan 04, 2022; accepted Mar 12, 2022

Abstract: Hybridization of natural and synthetic fibers has the ability to improve composite performance. It means that the combination of natural fibers such as coir, jute, bamboo, and sisal with synthetic or glass fiber can broaden the role of the composite material, especially for structural application. This study developed a finite element simulation to investigate the damage to the bow structure of the fishing boat hull, which was produced using hybrid coir-glass fiber composite (HCGFRP) material subjected to front collision load. The experimental measurement was conducted to determine the mechanical properties of four hybrid composite laminates defined based on the differences in their layers number, fiber types, and orientation angle. Moreover, a numerical simulation model was applied to the traditional fishing boat colliding with fishery harbor quay, and the scenario was defined by varying the boat speed and the types of laminates adopted on the hull structure. The results showed the damage level for the bow structure of the HCGFRP boat due to the collision accidents, while the numerical findings are expected to be used as the basic knowledge in applying the hybrid coir-glass fiber laminates composite as an alternative hull construction material.

Keywords: Boat collision, hybrid coir-glass fiber composite, bow structure damage, finite element analysis

***Corresponding Author: Ojo Kurdi:** Mechanical Engineering Department, Engineering Faculty, Diponegoro University, Semarang, Indonesia; Email: ojokurdi@ft.undip.ac.id
Aulia Windyandari: Mechanical Engineering Department, Engineering Faculty, Diponegoro University, Semarang, Indonesia; Industrial Technology Department, Vocational School, Diponegoro University, Semarang, Indonesia
Sulardjaka: Mechanical Engineering Department, Engineering Faculty, Diponegoro University, Semarang, Indonesia
Mohammad Tauviqirrahman: Mechanical Engineering Department, Engineering Faculty, Diponegoro University, Semarang, Indonesia

1 Introduction

Laminated fiber-reinforced polymer composite has been adopted widely in the marine industries due to its several advantages compared to steel, aluminum, and wood. It is commonly used for small craft vessels such as pleasure boats, yachts, patrol boats, fishing boats, fast ferries, and workboats. It is important to note that some of the factors generally considered in selecting an alternative material for boat construction include corrosion resistance, low thermal expansion, seamless hull, and high specific mechanical properties. Meanwhile, the polymer material is observed to have a lesser strength than metals, but a reinforced fiber can significantly improve its mechanical properties. Examples of synthetic reinforced fiber commonly used include carbon and glass fiber. However, natural fibers can be adopted as an alternative reinforced fiber because they offer biodegradable, renewable, and cheaper. Moreover, the limitations of natural fiber reinforced polymer composite can be improved through hybridization and special fiber treatment such as chemical, biological and physical treatments.

Natural fibers such as coir, jute, sisal, and bamboo are adopted as reinforced fibers in bio-composite material. Bio-composite material has offered a green boat building production process that can be considered as an alternative boat hull material by naval architects and boatyards. On the marine and manufacturing industry application, the investigation of biocomposite mechanical and physical properties should be conducted. Sen *et al.* [1] reviewed the mechanical properties of several natural fibers such as sisal, bamboo, coir, and jute fibers, and hybridization was discovered to have a significant influence on the tensile properties of the natural fiber composite. Moreover, sisal, coir, bamboo, and jute fiber-reinforced composite were observed to have high impact strength, moderate tensile strength, and flexural characteristics. The study also attempted to use natural fibers to solve the waste disposal problem, especially for developing countries with abundant natural fibers.

On the small craft and boat production with composite material, considerable progress has been shown on the

capability to build the complex boat structure with multi-material and withstand an extreme load. Shenoi *et al.* [2] also discovered that the use of polymeric composite material for marine structures increases due to its ability to produce a better safety and quality level. Moreover, the life cycle assessment of these composite structures is required to identify the environmental impact of their application. There is also the need to focus more on structural health monitoring to maximize, extend, and ensure the safety of the marine composite.

The hybridization of natural and synthetic fiber offers an attractive behavior and price for the composite structure due to its ability to combine the behavior of the single composite components, which is influenced by fiber length, chemical composition, matrix mechanical properties, and the fiber-reinforced treatment. Moreover, hybridization can improve toughness and impact strength [3, 4]. For example, Khalil *et al.* [5] showed the mechanical properties of hybrid oil palm empty fruit bunch (EFB)-glass fiber reinforced polyester composite and indicated the ability of the glass fiber to increase the strength and modulus of the hybrid composite. It was also discovered that more glass fiber content led to better mechanical properties while an increase in the EFB escalated the fracture elongation of the composite produced.

Several studies on the hybrid natural and synthetic fiber have also been conducted concerning kenaf and carbon fibers [5], basalt flax and synthetic fiber (glass/carbon) [6–9], jute and glass fiber [10, 11], sisal, and glass fiber [12], bamboo and glass fiber [13–15], sugar palm yarn and glass fiber [16], coir and glass fiber [17], as well as EFB and glass fiber [5, 18]. It was discovered that the mechanical properties of the hybrid natural and synthetic fiber composite were increased due to the inclusion of glass/carbon fiber. Moreover, substituting 15% of glass fibers with natural fibers can be achieved without changing the material's mechanical properties but improving flexibility and strain characteristics. The natural fiber quality and production procedure also influence the hybrid composite mechanical properties, such as stacking sequence, layering method, resin type, and fiber orientation angle.

The hybrid composite has been adopted for engineering construction because the combination generates better mechanical properties such as tensile, flexural bending, creeps, bending, and impact strength [19–22], thereby making it applicable in the field of marine engineering and structures. Moreover, the lignocellulosic fiber composite fascinated marine engineers and scientists to develop green material as a surrogate of carbon steel or fiber synthetic composite material. This hybridization can improve and increase the durability of natural fiber composite subjected to physical, chemical, and biological deterioration. Furthermore, the increased aging resistance and better mechanical stability associated with hybridization can reduce the low compatibility between hydrophilic fibers and hydrophobic resin. The hybrid composite can also compromise environmental issues, mechanical strength, production cost, and reliability [23, 24].

The application of the natural fiber and the hybrid composite as the boat hull material has been previously studied. For example, Misri *et al.* [25] investigated hybrid woven-glass and sugar palm composite as the surrogate of fiberglass boat material using unsaturated polyester as the resin or matrix. The production of the hybrid composite boat through the compression molding technique was also evaluated while the tensile and impact strength behaviors were tested based on the ASTM 5083 and ASTM 256 standard. The results showed that the tensile strength, failure elongation, impact strength, and young modulus increased significantly due to the inclusion of woven-glass fiber. Moreover, compression molding was recommended as the layering procedure of the hybrid woven-glass and sugar palm fiber composite for boat hull production.

Renjith and Nair [26] also conducted a structural analysis on a boat hull produced using natural fiber-reinforced polymer composite. Some of the natural fibers used include pineapple, jute, abaca, bamboo, banana, and waste silk, with their mechanical properties presented and compared. The results showed that the natural fiber composite could be used as a small boat hull material, while finite element analysis showed its safety factor is within the acceptable limit. Moreover, the waste silk composite was observed to have better mechanical properties than the others and was recommended for structural applications and construction.

Tikupadang *et al.* [27] also studied the tensile and flexural bending strength of *Agave Cantula Roxb* fiber composite as a hull material in fishing boats based on the fiber fraction composition of 0%, 20%, 30%, 40%, and 50%. The tensile and flexural bending tests were conducted in line with the ASTM D3039 and ASTM D790-03 standard, and the results showed the composite laminate with a fiber content of 50% had tensile strength and the maximum bending stress considered to have fulfilled the requirement of the Indonesia Classification Bureau standard for boat hull material.

Several previous studies have explored the mechanical characteristics and advantages of hybrid natural and synthetic fiber as a surrogate of common engineering material. However, there is limited research on the comprehensive assessment of the hybrid composite structural response to dynamic loads such as collision and impact. It is essential due to the need to evaluate the application of hybrid

composite for boat hull construction more than only the static load such as hull girder strength analysis, thereby leading to the conduct of collision analysis to assess the structural damage which can cause the loss of vessel hull water tightness due to excessive deformation. Furthermore, there is limited study on assessing the permissible boat service speed in the harbor basin area, which is required to avoid serious hull structural damage and catastrophic incident during collision accidents.

This condition has motivated the development of the numerical damage analysis for the bow structure of the hybrid coir-glass fiber composite fishing boat. The process involved determining the mechanical properties of the hybrid coir-glass fiber-reinforced polyester polymer (HCGFRP) through an experiment, while the defined material model was validated by comparing the numerical bending deformation with the experiment results. The collision scenario was also defined at different service speeds, laminate types, and thicknesses. It is important to note that the essential contribution of this research is to determine the damage level of the boat structure produced using hybrid coir-glass fiber-reinforced polymer due to the collision load and investigate the performance of the HCGFRP material as a surrogate of fiberglass composite using the nonlinear finite element analysis.

This article is structured into several sections, with Section 1 indicating the background and introduction of this study. Section 2 describes the experimental and mechanical properties of the hybrid coir-glass fiber-reinforced polymer. Then, Section 3 presents The HCGFRP material modeling and validation conducted by comparing the numerical and experimental results of the bending deformation due to the defined lateral load. The description of the fishing boat adopted for the collision simulation analysis is presented in Section 4. While Section 5 reports the numerical simulation analysis results for the defined collision scenario, and Section 6 presents the conclusion and summary.

2 Experimental study and the mechanical characteristics of the hybrid coir-glass fiber-reinforced polyester polymer (HCGFRP) composite

2.1 Experimental study

Experimental studies were conducted on HCGFRP materials using appropriate instruments or equipment to obtain the mechanical properties of each specimen, such as the tensile, bending, and impact tests. Moreover, a series of mechanical tests were also conducted to determine the mechanical characteristics such as tensile strength, flexural strength, and impact strength. The results were processed to obtain a numerical model to represent the mechanical properties of the HCGFRP composite material.

Coconut fiber was used as the core material and placed right in the middle of the lamina/core of the HCGFRP material lamination process in the specimen, and this is necessary because the core usually receives a lower voltage load compared to the top and bottom layers. This configuration was able to optimize the material's strength, considering that the layer with the potential to receive the most significant load was supported by a laminate made of glass fiber which has more substantial mechanical characteristics when compared to the coconut fiber. This coating

Table 1: Laminate type configurations in layers number, stacking sequence, and fiber orientation angle

Specimen type	Layers number	Stacking sequence	Fiber orientation angle
Type 1	5 layers	mat300/wr600/Coir Fiber/ wr600/mat300	random / 0°/Core / 0°/ random
Type 2	5 layers	mat300/wr600/Coir Fiber/ wr600/mat300	random / 45°/ Core / 45°/ random
Type 3	9 layers	mat300/wr600/ mat300/wr600/Coir Fiber/ wr600/mat300/ wr600/mat300	random / 0° / random / 0° / core / 0°/ random / 0° / random
Type 4	9 layers	mat300/wr600/ mat300/wr600/Coir Fiber/ wr600/mat300/ wr600/mat300	random / 45° / random / 45° / Core / 45°/ random / 45° / random

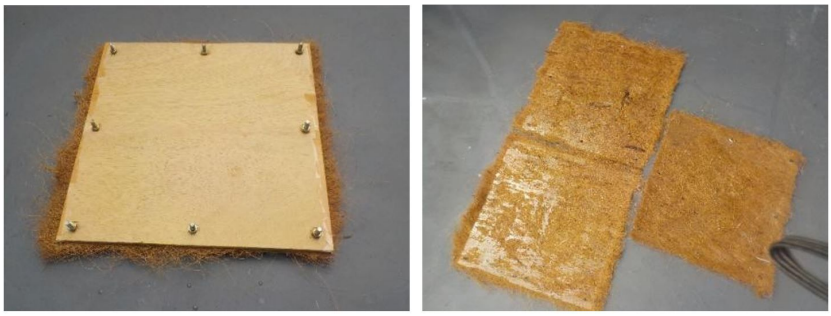

Figure 1: The process of making coconut fiber sheets

Figure 2: Lamination process using the hand lay-up method to manufacture hybrid coir and glass fiber composite material (HCGFRP)

technique is commonly known as sandwich lamination. Meanwhile, the configuration of the laminate type for each specimen is presented in Table 1.

The production of the hybrid specimens of coconut and glass fibers was initiated by producing sheets from the coconut fiber through pressure and a little resin liquid to bind the coconut fibers together, as indicated in Figure 1. The resin was not poured completely to ensure it enters the crevices of the coconut fiber during the process of manufacturing hybrid materials after it has been used to form the sheets. This technique is expected to produce a hybrid composite material consisting of both glass and coconut fibers thoroughly bonded through resin at the same time.

The hybrid composite material was produced using a hand lay-up lamination technique, usually employed to produce fiberglass ship hulls in shipyards. The lamination started with the application of liquid resin as the initial base, after which wr600 and mat300 fiberglass fibers were inserted, and resin applied again. Moreover, the coconut fiber was placed right at the middle of the lamination process conducted according to the fiber configuration described in the previous sub-chapter, with the steps used for the inner coating highlighted in Figure 2. The pressure was also applied using a glass sheet to ensure the resin was absorbed thoroughly into the crevices of the coconut and glass fibers, and this was used to represent the pressing process in the ship's hull manufacturing process using rolls to ensure the standard amount of pressure was provided and that the resin also fill the gaps in the reinforcing fibers.

The specimen's dimensions used for the tensile test were in line with the thickness of the specimen and the ASTM D3039/D3039M-00, Figure 3. The tensile and bending testing processes were conducted using a universal testing machine with a maximum tensile capacity of 1000 KN with the rate of stretching regulated by the size of the hydraulic valve opening that drives the machine's piston. Moreover, the maximum strain rate was achieved when the hydraulic valve was opened maximally.

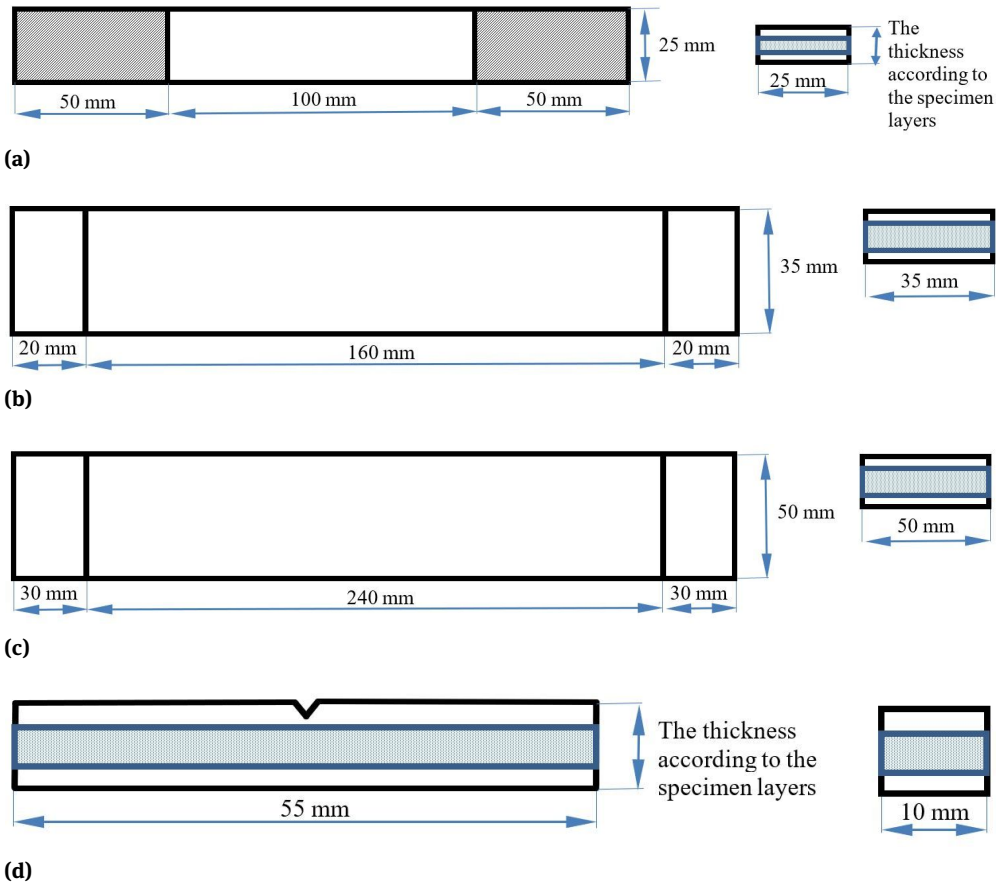

Figure 3: Dimensions of the test specimen according to the test standard: (a) Tensile test – ASTM D3039; (b) Bending test for 5 layers-ASTMD790-03; (c) Bending test for 9 Layer-ASTM D790-03; (d) Impact test/Impact-ASTM D5942-96

2.2 Mechanical properties of the hybrid coir-glass fiber-reinforced polymer (HCGFRP) composite

Figure 4 shows that the highest tensile strength of 76.55 MPa was achieved in type 3 lamina configuration, with eight layers of glass fiber compared to the four layers in lamina types 1 and 2. It also has better tensile strength than type 4, which has the same number of layers due to the orientation angle of its glass fibers. It means that the addition of glass fiber at orientation angles of 0° and 45° in HCGFRP for type 3 can increase the tensile strength by 2.89% and 22.45%, respectively. At the same time, those with 5 and 9 layers increased by 39.72% and 17.4%. This characteristic pattern also showed that the tensile strength of the HCGFRP material could be improved by increasing the number of layers of glass fiber. However, the percentage increase is strongly influenced by the quality of the lamina due to the process involved in its production.

The effect of the configuration of the laminate type on the tensile strain is presented in Figure 5, with those having

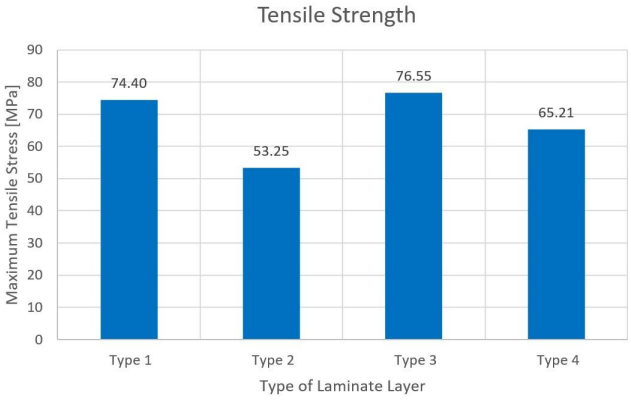

Figure 4: Characteristics of the tensile strength of HCGFRP in each configuration of the lamina

a higher number of glass fibers discovered to have a higher tensile strain value with an increase in the magnitude by 13.45% and 28.33% for 0° and 45° orientation angle respectively. Meanwhile, the solid tensile strain at 0° angle was found to be greater than 45°, and the decrease in tensile strain was recorded to be 23.8% and 13.8% for those with

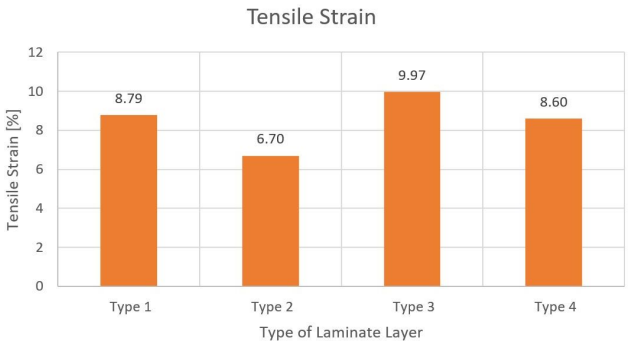

Figure 5: Tensile strain characteristics of HCGFRP in each lamina configuration

Figure 6: Fracture contour in tensile test specimen

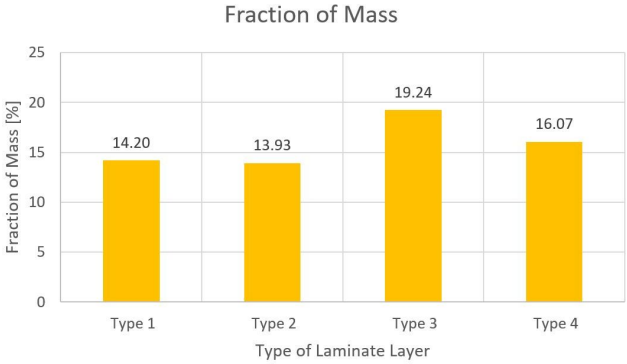

Figure 7: Mass fraction of HCGFRP in each lamina configuration

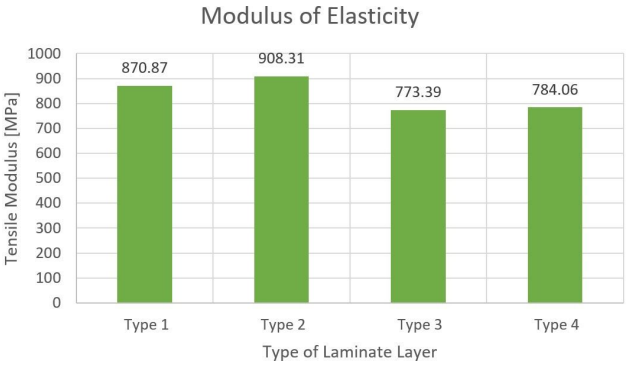

Figure 8: Modulus of elasticity of HCGFRP in each lamina configuration

five layers and nine layers, respectively. The results showed that the addition of glass fiber could increase the tensile strain value and cause the material to be more flexible or elastic. It means that the strength of the HCGFRP material is dominated by the matrix and shear strength between the laminae layers. Moreover, the tensile test results showed the fracture of the material started with the delamination phase, as indicated in Figure 6, which occurred due to the shear stress caused by the differences in elongation associated with the variations in the level of stiffness of the core lamina (coconut fiber composite) and top/bottom lamina (glass fiber composite). It was also discovered that the tensile strain characteristics of the 9-layer laminate type specimen become more flexible or elastic despite the increase in the mass fraction, as indicated in Figure 7. The imperfection in the lamination process conducted using the hand lay-up method was the reason for the inability to form a good bond between the fiber and the resin, thereby making the additional layer that is expected to allow the HCGFRP material to be more rigid to become more flexible.

The tensile strength and strain characteristics were used to determine the magnitude of the modulus of elasticity of each type of lamina, as indicated in Figure 8. It was discovered that the lamina type with the enormous tensile strain has the smallest modulus of elasticity as indicated by the findings that the modulus of elasticity at the orientation angle of 45° is greater than 0° for the same number of layers. Moreover, the lamina with five layers was also found to be larger than those with nine layers at the same orientation angle.

The tensile test results also showed that the mechanical characteristics of HCGFRP are significantly affected by the number of layers and angle of orientation of the glass fiber. It was indicated by the fact that the higher amount of glass fiber had increased tensile strength in the range of 2.89% – 22.45%, and this was explained to be due to the high tensile strength mechanically contributed by the glass fiber to the HCGFRP material. It means that it is possible to adjust the magnitude of tensile strength needed in the HCGFRP using the mass/volume fraction of the glass fiber content in the composite.

The orientation angle was also found to affect the tensile strength with the sample at 0° observed to have better strength than those with 45°. It is explained by the fact that the tensile load acting on the specimen's cross-section at 0° is directly resisted by the glass fiber with the same direction

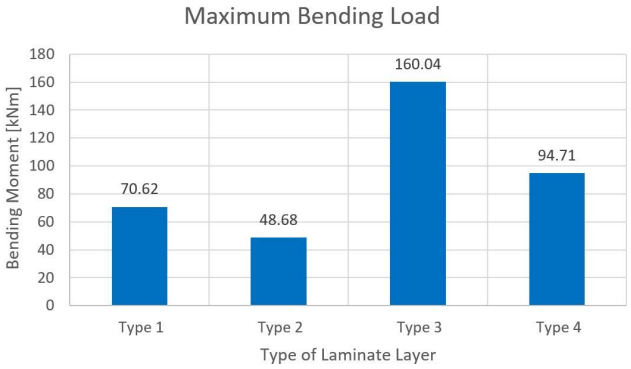

Figure 9: Maximum bending load of HCGFRP in each laminate

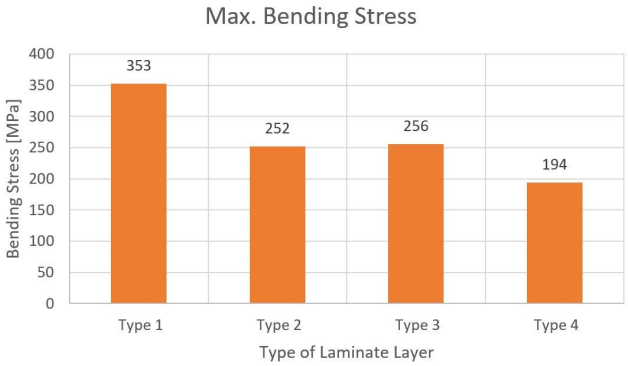

Figure 10: Maximum bending stress of HCGFRP in each laminate configuration

of force, thereby making the stress refuted in its entirety by the strength of the reinforcing fiber. Meanwhile, at 45°, the tensile load was supported by the reinforcing fiber with a deviation angle of 45°. It means that the load was not refuted with the full strength of the reinforcing fiber. Another essential factor that is needed to be considered is the quality of the lamination process while producing the HCGFRP composite materials. This phenomenon was shown by the dominance of the mechanical characteristics of the specimens with the matrix.

The bending test was used to obtain the mechanical characteristics such as the maximum buckling load, maximum bending stress, and flexural modulus. The buckling test showed that the maximum bending load was at the lamina with nine layers and 0° orientation angle, as indicated in Figure 9. It was predicted using Type 3, which had the highest specimen thickness and required a more significant bending moment to be bent. However, it was discovered that Type 1 has the highest bending stress, as indicated in Figure 10, which means the higher number of layers led to a reduction in the maximum bending stress. It is associated with the imperfections allowed in the lamination process of samples having more layers in the hand lay-up method, thereby reducing the effectiveness of the reinforcing fiber added and limiting its ability to increase the maximum bending stress directly. configuration

The maximum bending load and stress were used to determine the flexural modulus, and the highest value was recorded in the type 1 lamina configuration as indicated in Figure 11, while the 5-layer lamina had the highest flexural stiffness. The lower number of layers indicates that glass fiber reinforcement is more effective at increasing the strength of the HCGFRP composite. It is, however, essential to note that a small number of coatings can reduce the potential for imperfections in the lamination process to ensure the material has a higher flexural modulus.

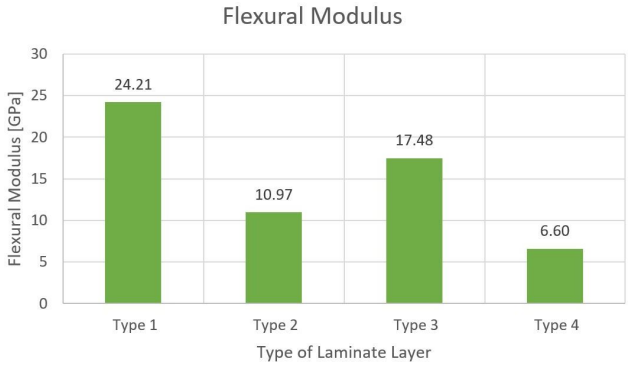

Figure 11: Flexural modulus of HCGFRP in each lamina configuration

The HCGFRP material included in the orthotropic was observed to have a different modulus of elasticity from the bending test (flexural modulus) compared to the value recorded from the tensile test (tensile modulus). It is associated with the mechanical characteristics of the composite specimens' upper, lower, and middle layers, which are very likely to occur, especially in composites reinforced with fibers that have random orientations such as coconut and chopped strand mat-type glass fibers.

The last mechanical test was on impact, and the 9-layer glass fiber laminate with 0° orientation was found to have the most significant impact energy, as indicated in Figure 12. It means the number of laminae significantly affected the impact energy of HCGFRP as indicated by the 321% and 313% increment recorded at 0° and 45° orientation angles, respectively, as the layers increased. Meanwhile, the other glass fiber orientation angles did not significantly differ on the same number of layers, but 0° was discovered to have better impact energy compared to 45°. The same trend was also recorded for impact toughness, as indicated in Figure 13.

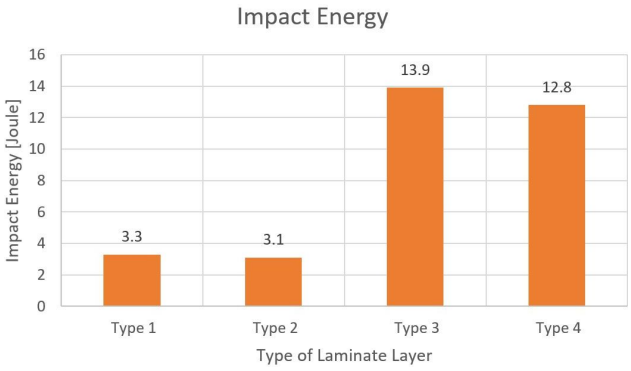

Figure 12: The impact energy of HCGFRP on each lamina configuration

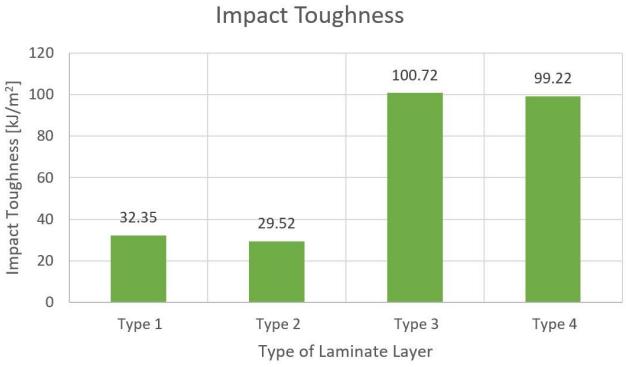

Figure 13: Impact toughness of HCGFRP in each lamina configuration

3 Hybrid coir-glass fiber-reinforced polyester polymer (HCGFRP) composite material model and validation

3.1 HCGFRP composite material model

The HCGFRP material has two types of laminae which are the top/bottom layer (Top and Bottom layer) produced using glass fiber laminate (GFRP) and the core or middle layer (Coir Fiber) laminate. Based on the commonly used approach [28], it is assumed that the mechanical characteristics of each lamina are homogeneous and are modeled as linear elastic orthotropic materials. Moreover, there are four types of laminates in the HCGFRP composite material developed, and they were varied based on the number of layers, types, and orientation angles of the glass fiber, as indicated in Table 1. It is, however, essential to note that the orientation angle and fiber direction have the same position in the longitudinal direction for all the types and transversely to identify the mechanical characteristics of the material as transversely isotropic. Therefore, it was assumed that they all have the same mechanical properties in the X and Y axes, which were measured only in one direction.

The behavior of the HCGFRP material was modeled as an ideally plastic material up to the moment it experienced a brittle fracture. Moreover, the damage simulation was defined through the damage evolution using the DISPLACEMENT TYPE, which involves determining the evolution of the damage based on the total or plastic displacement after the occurrence of the initial damage (Initiation Damage). The details of the mechanical properties used in the simulation are presented in Table 2.

Table 2: Properties of the materials used in the FE Model

	Type 1	Type 2	Type 3	Type 4
Young modulus (GPa)	24.212	10.974	17.482	6.601
Poisson ratio	0.3	0.3	0.3	0.3
Yielding stress (MPa)	40.29	36.65	31.7	34.17
Density (Kg/m^3)	1364	1240	1180	1560
Fracture strain	0.088	0.067	0.0997	0.086
Stress triaxiality	1.35	1.30	1.32	1.33
Strain rate	1	1	1	1
Damage evolution	Type displacement, softening linear, degradation maximum	Type displacement, softening linear, degradation maximum	Type displacement, softening linear, degradation maximum	Type displacement, softening linear, degradation maximum
Fracture energy (Joule)	3300	3100	13900	12800

3.2 Bending test simulation for material model validation

The material model from the experiment was validated by comparing the simulation results with data from the experimental study. It is important to note that the bending test was selected as an object for the validation, and this is because lateral loads dominate the majority of structural problems in ship structure analysis. It means that the structure's response to these loads is very relevant and is represented by the response of the plate in the bending test process. Therefore, the modulus of elasticity used in the material model was obtained from the elastic modulus data obtained from the experimental measurement.

The bending test model used 1800 elements of 4 quadrilateral vertices with a total of 1920 vertices, as indicated in Figure 14. This number of nodes was determined according to the values needed to calculate the accuracy to produce a convergent computational process. The model's thickness was also adjusted to the thickness of the bending test specimen for each type of HCGFRP laminate. At the same time, the boundary conditions were adjusted to the support characteristics from the bending test, which was simply supported. Moreover, the distance between the supports was also adjusted to the distance of the supports in the bending test.

A concentrated load acting at an independent point on a multi-point constraint (MPC-RBE2) was also used because the bending experimental data produced the maximum magnitude of the concentrated load of the system. This concentrated load was later distributed through the press on the bending test machine with the end of the pressure tool that distributed the load force represented by nodes connected rigidly at one independent point in the multi-point constraint modeling system (MPC-RBE2), as indicated in Figure 15.

Figure 14: Bending test model for material model validation

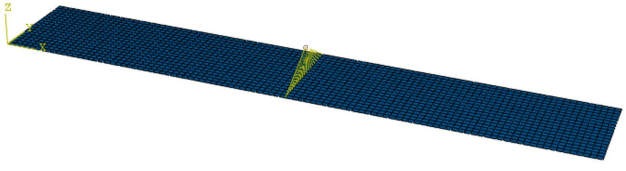

Figure 15: Multi-point constraint type RBE-2 for load model in bending test simulation

The defined model was run using two algorithms with different computational methods. The first was the linear perturbation static method, which assumed that the material was linearly elastic and that the plasticity was not considered. At the same time, the second was the general static method which considered the plasticity of the material and was observed to be very appropriate for cases of structural response undergoing considerable deformation or large displacement problem, which generally has permanent or plastic deformation. This problem can also be identified as a nonlinear problem. Meanwhile, the computational simulation results of the two methods were later compared with the experimental data of the bending test.

The experimental data used for the model validation was the displacement value when the specimen was subjected to the maximum compressive load. Meanwhile, the maximum force and thickness of the specimen used in each simulation model are presented in Table 3. It is important to note that the displacement data for each specimen were obtained by photographing. The deformation point was determined by digitizing the data points through a digitizer plot, and the ordinates generated were transferred to Microsoft Excel to obtain the deformation shape of each specimen.

The simulation model developed was run using the ABAQUS software, and the results were in the form of the deformation distribution on the test specimens obtained through the linear perturbation and general static methods as indicated in Figures 16 and 17, respectively. The data were further compared with the displacement data of the bending test experiment, as shown in Figures 18–21.

The results showed that the general static method had better deformation estimation than the linear perturbation method. It is associated with data in this method to describe the phenomenon of plasticity in the case of structural deformation. Moreover, Figure 18 shows the maxi-

Table 3: Compressive force load data and specimen thickness for bending test simulation

Laminates type	Maximum compressive force [N]	Specimen thickness [mm]
Type 1	10300	10.0
Type 2	9730	11.5
Type 3	11640	13.0
Type 4	11350	15.1

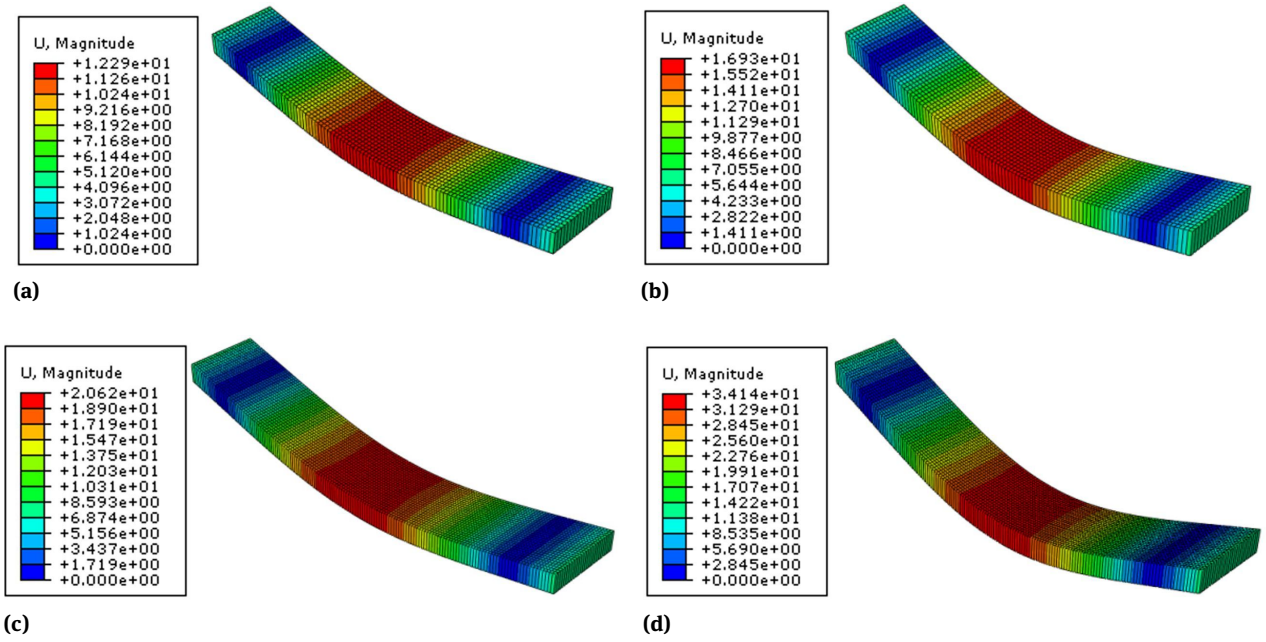

Figure 16: Estimation of deformation through linear perturbation method (linear elastic): (a) laminate type 1, (b) laminate type 2, (c) laminate type 3, (d) laminate type 4

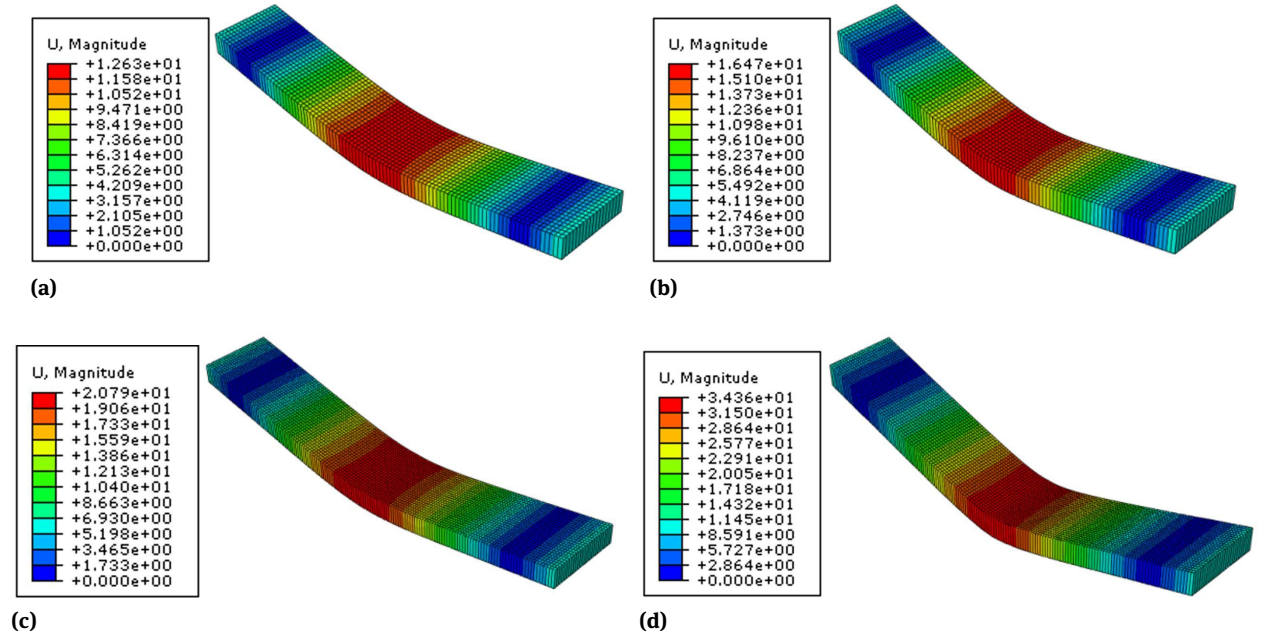

Figure 17: Estimation of deformation through general static method (with plasticity): (a) laminate type 1, (b) laminate type 2, (c) laminate type 3, (d) laminate type 4

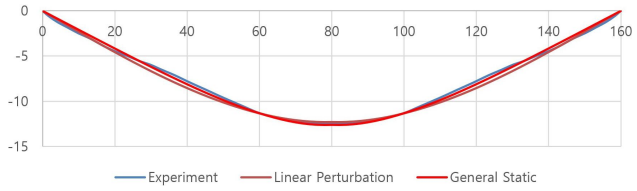

Figure 18: Comparison of bending deformation values on laminate type 1

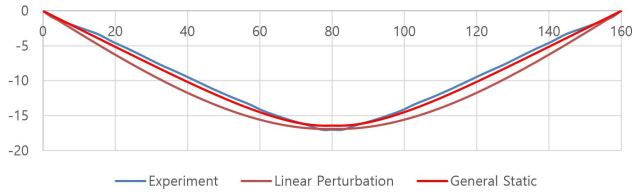

Figure 19: Comparison of bending deformation values in laminate type 2

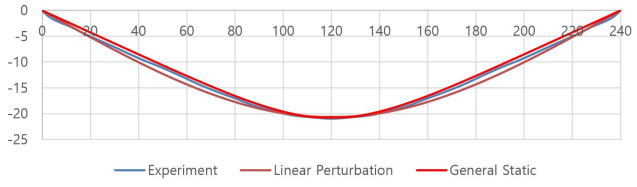

Figure 20: Comparison of bending deformation values on laminate type 3

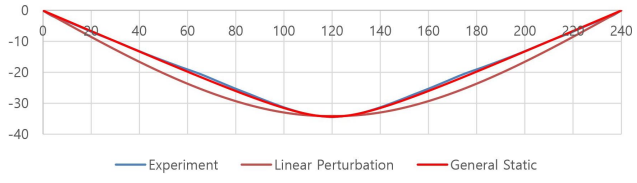

Figure 21: Comparison of bending deformation values on laminate type 4

mum deformation value of laminates type 1 ranging from 12 mm and has a ratio of 7.68% between maximum deflection and unsupported length (deflection span ratio). The linear perturbation method was observed to have shown an excellent estimation at a relatively small maximum deformation value with a deflection span ratio value below 10%. However, it produced a deformation of the beam (beam curvature), which is slightly different from the experimental results in cases with relatively large deformation values (deflection span ratio >10%), such as laminate type 2 with 10.6% and type 4 with 14.2%. Meanwhile, the general static method showed that the estimation of the beam deformation curvature is excellent and almost coincides with the beam deformation curvature from the experimental data. It means the definition of material plasticity in the HCGFRP material model can influence the accuracy of the deformation shape in the simulation model.

These findings indicate that the HCGFRP material model from the experiment could produce an accurate estimate of the maximum deflection value as indicated by the numerical calculations conducted using linear perturbation and general static methods. The model also showed excellent results for estimating the shape of the deformation curvature, especially in the general static method. In contrast, the decreasing level of accuracy in the linear perturbation method was associated with the exemption of the plasticity of the material in the calculation algorithm procedure. It can, therefore, be explained that the response of the model structure is assumed to be linearly elastic in this method.

The validation process also showed that the material model developed can represent the HCGFRP material in the simulation to evaluate its performance when used as a ship hull material. It was indicated by the excellent validity recorded with two different numerical computational methods. It concluded that the model could be used to determine the response characteristics of the ship's structure which is a feasibility study associated with the application of HCGFRP as a hull material.

4 Ship description for simulation model

Traditional fishers mainly use traditional fishing boats to conduct fishing activities, and their hulls are majorly constructed using wood. It is, however, essential to note that the quantity of wood materials usually used to construct these traditional ships is not balanced with the time required to supply the woods. For example, the extensive woods that generally require more than ten years to grow are mainly used for ship construction, leading to the scarcity of resources and an increase in the price of wood. Moreover, the government has also imposed restrictions on the exploitation of timber commodities to maintain forest sustainability. Therefore, the government directed traditional ship artisans to use alternative materials to substitute for wood due to the limited availability and the high cost of wood commodities.

Several alternative materials have been widely used for ship hulls, such as glass fiber-reinforced polymer (GFRP), high-density polyethylene (HDPE), polyvinyl chloride (PVC), aluminum, Ferro cement, and others. The HCGFRP composite material developed and described in the previous sub-chapter was studied and evaluated for its

feasibility and reliability when used as a ship hull material using simulation techniques to determine its strength and response after applying it.

A ship and HCGFRP material model were required for the simulation, and the ship selected is a traditional purse seine-type fishing vessel usually found on almost all the coasts in Indonesian waters with different types of hulls created by the ship artisans in each region. The variation in the forms of traditional purse seine hulls led to the selection of the rod type, which is observed to be the most common in the North Coast of Central Java Province. This type is an encircling fishing vessel that uses purse seine nets to catch a large volume of schooling fish, and this means it requires a large loading capacity. Therefore, it shows it has the large and appropriate size to evaluate the application of the HCGFRP as a hull material.

Table 4: The principal dimension of Batang type traditional purse seine vessels

Principal dimension	
Length overall (Loa)	30 m
Length of waterline (Lwl)	24 m
Length between perpendicular (LBP)	23.16 m
Breadth (B)	8.2 m
Draught (T)	2.6 m
Height (H)	3.6 m
Service speed (Vs)	15 knot
Displacement (Δ)	348.6 Ton
Block coefficient	0.662
Midship coefficient	0.976
Waterplane coefficient	0.892
Prismatic coefficient	0.678

Traditional purse seine ship designs have been passed down from generation to generation, with the construction process conducted based on the habits and references applied directly without using drawings and manufacturing procedures planned in a systematic and detailed manner. Therefore, the ship's hull dimensions and the design drawings were conducted after the ship was completed. However, it is essential to inform that the hull's principal dimensions were retrieved from Taury and Zakki [29], as indicated in Table 4 and the 3D diagram presented in Figure 22.

The construction of purse seine-type fishing boats was modified from wooden materials to a design with fiberglass. It is important to note that the dimensions of the structural members were not in line with the regulatory standards of the Indonesian Classification Bureau, especially regarding the thickness of the HCGFRP plate. However, the thickness

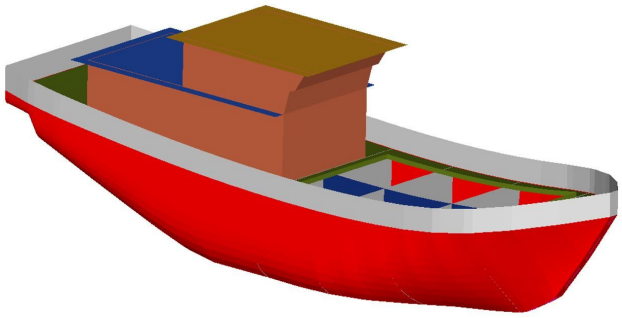

Figure 22: 3D geometry design of Batang type traditional purse seine hull

dimensions of each lamina type were studied for mechanical characteristics, and material models were applied. It was due to the assumption that the simulation was only conducted to assess the feasibility and reliability of the laminate type developed and not to design a new construction system for ships using HCGFRP material. This consideration was very relevant because the existing regulations do not stipulate the standard dimensions for the structural members of ships produced using new materials such as HCGFRP.

The structural design in the simulation model used a transverse construction system with the side of the hull reinforced using the mainframe with a distance of 1 m. Moreover, there is an elongated bulkhead separating the fish hold from the port side and the starboard side in the middle

Table 5: Structural Members of the Ship Framing System Model

No	Components	Dimension [mm]	Type
1	Main frame	200×Tl×350×Tl	Closed-bar
2	Center girder	500×Tl	Flat-bar
3	Side girder	500×Tl	Flat-bar
4	Deck girder	500×Tl	Flat-bar
5	Deck beam	200×Tl×350×Tl	Closed-bar
Tl = thickness of each laminate type, Table 6			

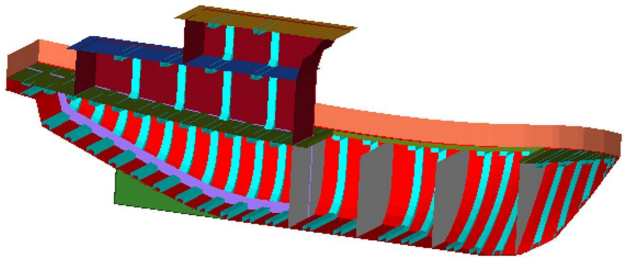

Figure 23: The frame structure design of the ship simulation model (without longitudinal bulkhead)

Table 6: Scenarios of ship and harbor quay collision simulation

No	Collision scenario	Laminates type	Laminates thickness	Service speed
1	Scenario 1	Type 1	10 mm	3 knot
2	Scenario 2			4 knot
3	Scenario 3			5 knot
4	Scenario 4	Type 2	11.5 mm	3 knot
5	Scenario 5			4 knot
6	Scenario 6			5 knot
7	Scenario 7	Type 3	13.0 mm	3 knot
8	Scenario 8			4 knot
9	Scenario 9			5 knot
7	Scenario 10	Type 4	15.1 mm	3 knot
8	Scenario 11			4 knot
9	Scenario 12			5 knot

of the loading room while the engine room was constructed using the same frame spacing, but the bottom section side girders were added as reinforcement for the engine mount. The details of the structure size and design of the framing system are presented in Table 5 and Figure 23.

5 The collision analysis of the HCGFRP fishing boat

This collision analysis was conducted to determine the structural response behavior in the case of the ship striking a pier. The analysis is necessary to identify the level of damage to the ship's bow structure, focusing on the damage having the potential to cause a leak that can sink the ship. Another analysis was also conducted to determine the speed limit of ships in the port waters to reduce the occurrence of catastrophic collisions, which can sink ships and cause loss of lives.

The simulations were defined based on the scenarios presented in Table 6, which were varied in line with the collision speed and the type of laminate used for the ship structure. Moreover, the model materials were assumed to be transversely isotropic even though composite materials are usually considered orthotropic. This assumption is relevant because the orientation angles of the reinforcing fibers were set at 0° and 45°and this placed the tensile strength value of the material in the same orthogonal axis direction. The initial velocity in the model was also determined using a set of nodes on all the nodes in the ship model to collide with a rigid wall or pier at an angle of collision set at 90°,

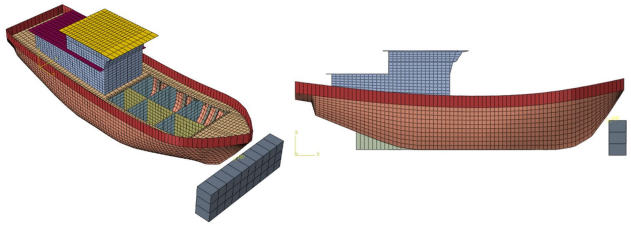

Figure 24: Geometric model of ship and harbor quay collision simulation

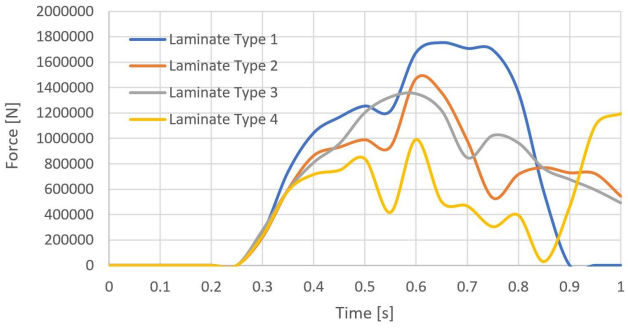

Figure 25: Force – Time of each type of laminate based on impact with a speed of 3 knots

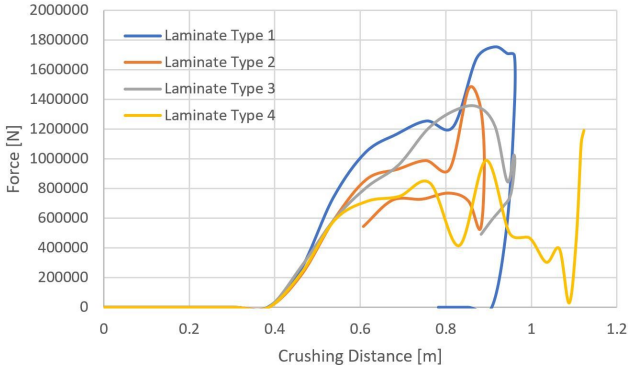

Figure 26: Force – displacement of each type of laminate based on impact with a speed of 3 knots

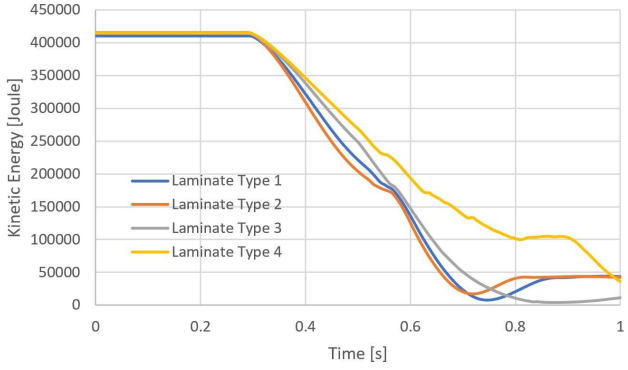

Figure 27: Kinetic Energy – Time of each type of laminate based on impact with a speed of 3 knots

known as a lateral collision. This angle was selected because it provides the greatest impact momentum compared to other angular conditions.

The numerical method used in the computational process was the penalty method, which subtracted the amount of contact force applied to the ship model (slave element) from the force required to restore the slave element node position when penetrating the dock model node formation (master element). Moreover, the magnitude of the contact force was influenced by the damping and penalty constant values selected automatically by the ABAQUS/Explicit due to the assumption that the defined simulation model has hard penalty contact characteristics which do not allow any node to pass through the master surface. This condition was observed to be suitable for ship collision cases where the ship constructed was not allowed to penetrate the pier or rigid wall, as indicated in the geometric model of Figure 24.

The complexity of the actual system was reduced through several simplifications made in the simulation model to save and reduce computational time. For example, the hydrodynamic effect of the fluid (seawater), especially on the behavior of the ship's motion after experiencing a collision, was not considered because its calculation process involves complex computational algorithms and is very expensive (very long calculation time). Furthermore, the simulation was focused on determining the effect of the laminated HCGFRP material on the performance of the ship structure. It is also important to note that the distance between the ship and the pier was shortened to reduce the computational time required to simulate the collision phenomenon.

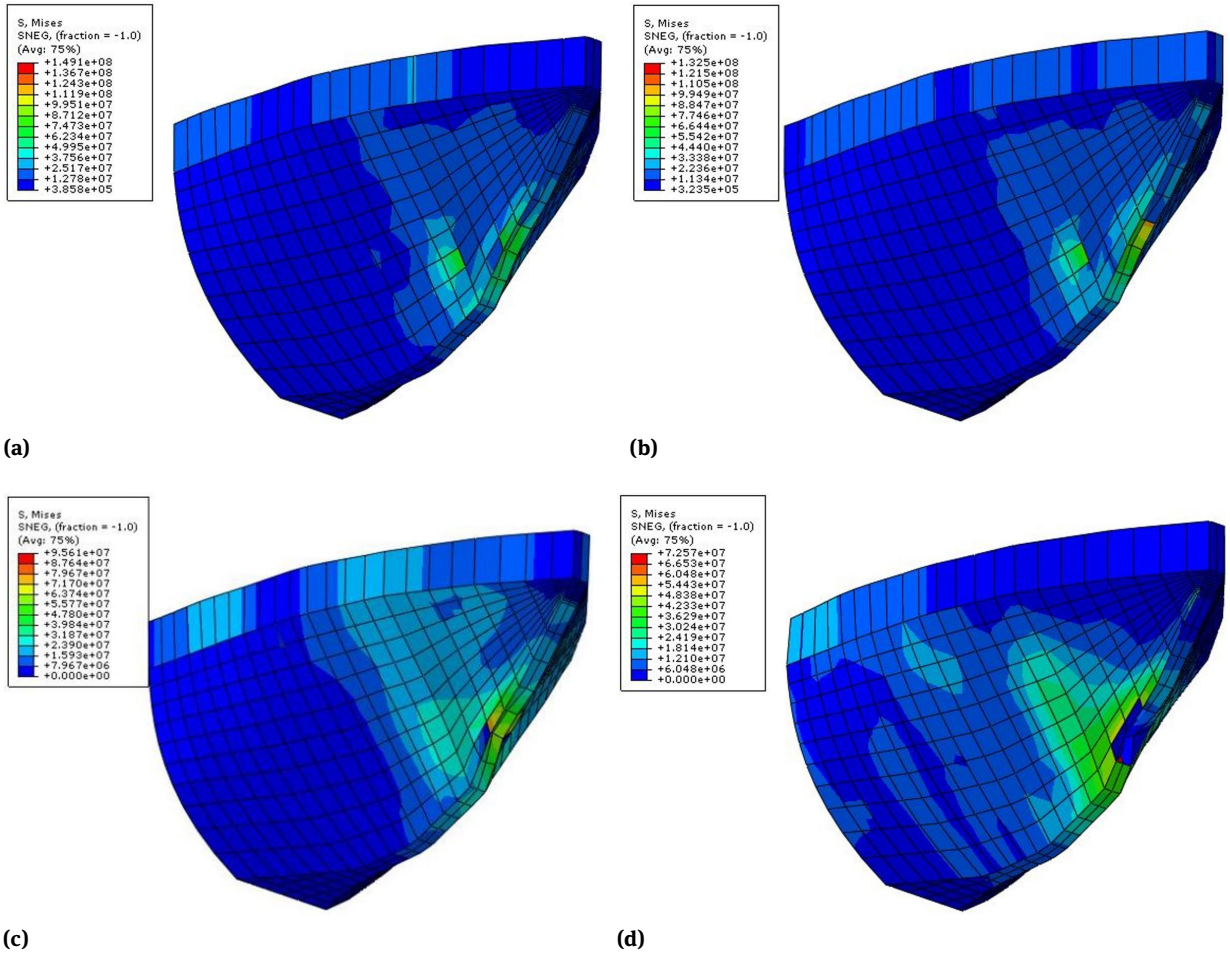

Figure 28: Deformation of the hull construction due to impact at a speed of 3 knots: (a) Laminate type 1, (b) Laminate type 2, (c) Laminate type 3, (d) Laminate Type 4

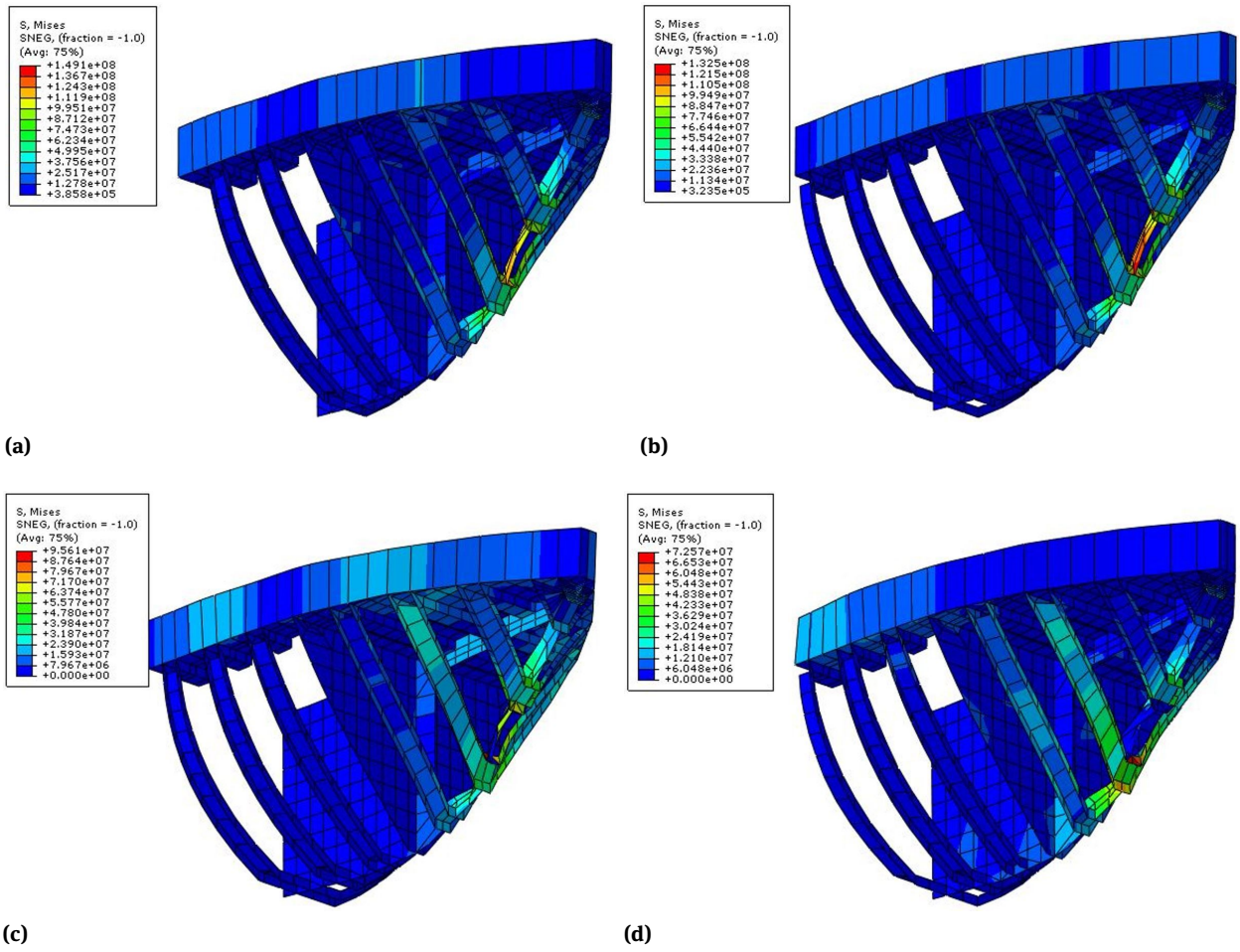

Figure 29: Deformation of bow construction due to impact at a speed of 3 knots: (a) Laminate type 1, (b) Laminate type 2, (c) Laminate type 3, (d) Laminate type 4

5.1 Fishing boat – harbor quay collision in service speed 3 knot

The simulation results at the service speed of 3 knots in Scenarios 1, 4, 7, and 10 are presented in Figures 25–29. The magnitude of the contact force and time presented in Figure 25 showed that Laminate type 1 could absorb collisions better than the other types of laminations as indicated by the reduction and absence of contact force at 0.9 seconds which means the ship retreated backward and did not touch the pier. It was confirmed by the contact force and impact distance graphs in Figure 26, where the type 1 lamina ship was observed to have moved backward after moving forward by 0.93 m. The lack of contact force indicates no part of the ship's bow has contact with the pier, but a contact force was recorded in laminate types 2 and 3 even though the ship has also moved backward, which means the bow construction was in contact with the pier. Furthermore, laminate type 4 was the weakest, as indicated by the ship's forward movement up to the end of the simulation. Despite the appearance of a decrease in the magnitude of the contact force in Figure 25, the collision did not end because the contact force increased significantly. It means that additional bow construction components were damaged by having contact with the pier, as indicated in Figure 26, where the ship is observed to have a continuous movement forward up to the end of the simulation. Type 4 laminate failed to dampen the ship's collision at a speed of 3 knots, and this is also indicated in the magnitude of the ship's kinetic energy in addition to the contact force graph.

The magnitude of the change in the ship's kinetic energy when experiencing the collision is presented in Figure 27, and a significant decrease in kinetic energy was recorded at approximately 0.3 seconds. It served as the beginning of the reduction in the ship's speed due to collision, which was observed to be successfully suppressed in lami-

nate types 1, 2, and 3 that touched a number close to zero. The graph also explains that the ship has moved backward after the collision, in laminates types 1 and 2. However, it tended to stop in type 3 after the collision event. In the case of laminate type 4, the ship is still moving forward up to completing the simulation termination time.

The simulation results of the bow construction damage of the four laminate types are presented in Figures 28 and 29. They are all observed to have experienced deformation due to impact. The highest maximum effective stress was indicated in the laminate type 1, which means it is stiffer when compared to other types of laminate. It follows that it has the highest modulus of elasticity value of 149 MPa compared to the other laminates and has the smallest thickness, which was observed to have led to higher stress at the same load from the contact force.

The high effective stress observed was not the only indicator of material fracture, which can also be determined using the material's ultimate tensile strength and maximum fracture strain. The failure or fracture represented by material deletion was observed in this study based on the maximum fracture strain criteria, and this was indicated by the type 4 lamination, which has the smallest stress but suffered a fracture due to the maximum fracture strain limit HCGFRP have been achieved in the model.

The damage experienced in types 1 and 2 was hull deformation in the stem bar and some stiffeners of the bow structure, as indicated in Figures 28a and 28b. It means that the high stress recorded in these types did not cause the material to fracture because the value is below the flexural tensile strength and the maximum strain value was also below the maximum fracture strain limit value. Meanwhile, even though the stress in bow construction with types 3 and 4 was smaller than 1 and 2, fracture occurred because the maximum fracture strain limit was reached.

These simulation results showed that the ship hitting the pier at a speed of 3 knots can damage the bow construction section in the form of structural deformation and even fracture. It is important to note that the damages in the form of deformation cannot cause ship leakage, and this means it will still float and not be considered dangerous to passengers. Meanwhile, the fracture as indicated in types 3 and 4 can cause leakage, allowing water to enter the forepeak tank, but the boat is expected only to experience bow trim as long as the collision bulkhead construction is intact. It is indicated that the four types of laminate are safe and reliable during a ship-pier collision at a speed of 3 knots.

5.2 Fishing boat – harbor quay collision in service speed 4 knot

The characteristics of the ship-pier collision at a speed of 4 knots are presented in Figures 30–34. It was discovered from the contact force against time graph in Figure 30 that the bow construction of the ship is always in contact with the pier. It means that its body touches the pier until the

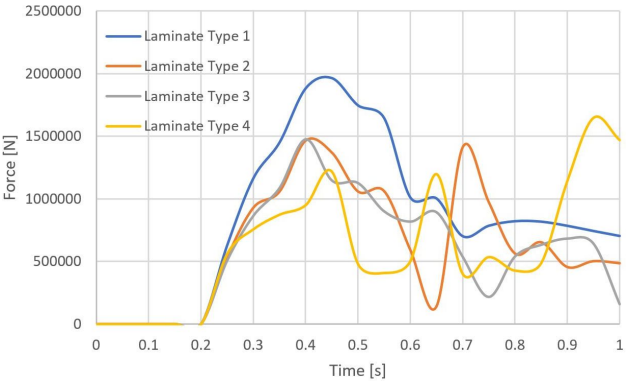

Figure 30: Force – Time of each type of laminate based on impact at a speed of 4 knots

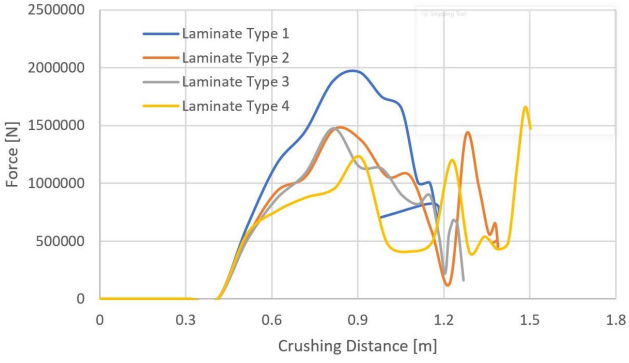

Figure 31: Force – displacement of each type of laminate based on impact at a speed of 4 knots

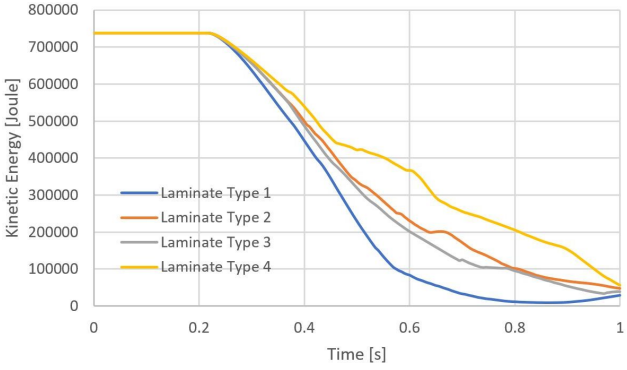

Figure 32: Kinetic Energy – Time of each type of laminate based on impact at a speed of 4 knots

simulation is finished. An increase in the speed of impact was observed to have caused the type 1 laminate and the bow construction of the ship not to stop hitting the pier, as indicated in Figure 31. The ship with the laminate type 1 was discovered to have struck forward at approximately 1.18 m. After that, the ship started bouncing to a distance estimated at 1m in front of the starting position. However, the bow construction was observed still stuck on the pier.

The kinetic energy graph presented in Figure 32 shows that the kinetic energy was nearly zero in the type 1 laminate while the other types only tend towards the zero point, and this means type 1 can reduce the kinetic energy of the ship faster than the others. It is similar to the previous explanation that the material's stiffness appears to be more influential in absorbing the ship's impact energy than the additional thickness of the laminate layer.

The degree of damage to the bow construction is presented in Figures 33 and 34, with the simulation results observed to indicate more severe damage due to an increase in the impact velocity. Type 1 had the smallest level of damage compared to the others, and it is also important to note that types 2 and 3 had no rips in the hull at a collision speed of 3 knots, but they both have tears at 4 knots. It means that an impact of 4 knots can cause hull leakage and allow water into the forepeak tanks.

The level of damage also increased in the bow structure. It can be seen on the extension of the damage, which was initially in the form of deformation in the stem bar to the bow structure, as shown in Figures 33 and 34. Moreover, the bow hull tear in the laminate type 4 was more expansive than before, as indicated in Figure 33d. The fracture damage in the stem bar was discovered to have occurred in all types of laminates. The increase in damage to the bow also showed the increased stress on the two bow frames that propagate to the collision bulkhead construction. There is also deformation in the deck area, especially in the bulwark, as presented in Figure 33d. It can be seen that the frame was pushed by the impact penetration, thereby leading to

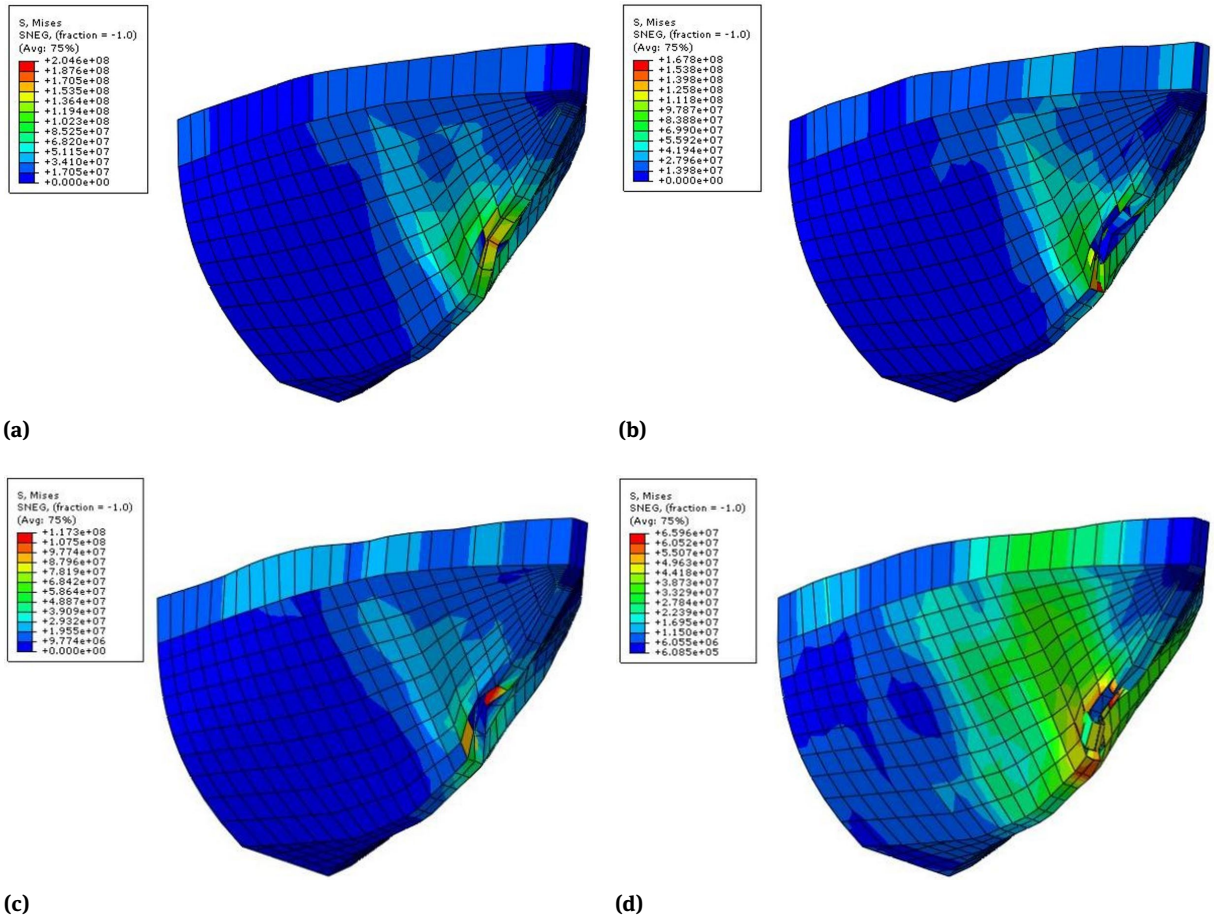

Figure 33: Deformation of the hull construction due to an impact at a speed of 4 knots: (a) Laminate type 1, (b) Laminate type 2, (c) Laminate type 3, (d) Laminate type 4

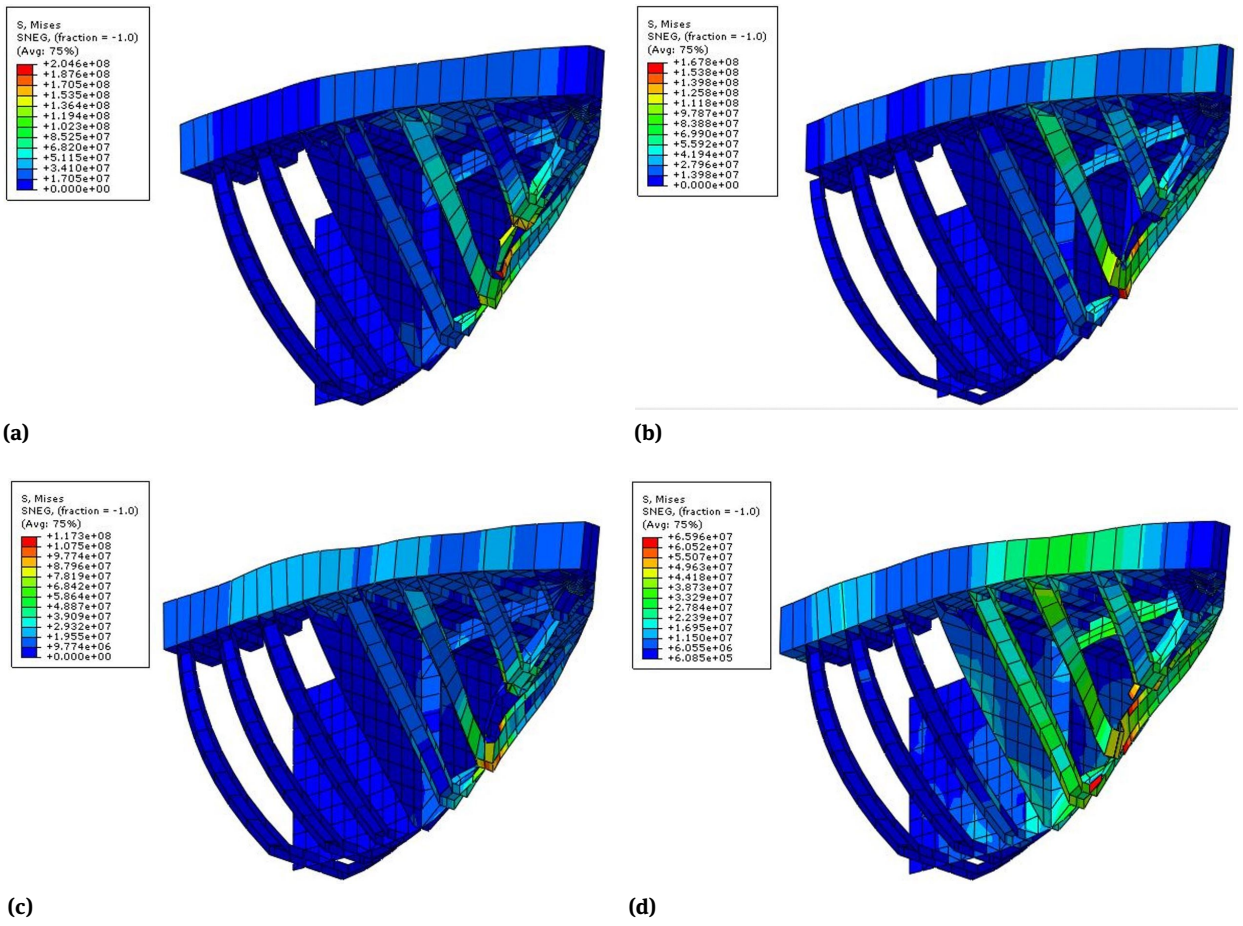

Figure 34: Deformation of the bow construction due to impact at a speed of 4 knots: (a) Type 1, (b) Type 2, (c) Type 3, (d) Type 4

the bending moments in the deck and bulwark. Meanwhile, even though the increasing level of damage caused the bow construction to lose its impermeability because the hull was torn, the ship was in a floating condition because the collision bulkhead was intact and did not experience any significant deformation. It means that the ship is afloat and safe at a collision speed of 4 knots and did not cause any fatal disaster.

5.3 Fishing boat – harbor quay collision in service speed 5 knot

The highest speed used to assess the impact strength of ships made from HCGFRP was 5 knots, and it was selected based on the assumption that it has at least half the ship's service speed when in the dock area. The graph showing the relationship between the contact force, time, and impact distance at this speed indicates all the laminate types have contact forces up to the completion of the simulation

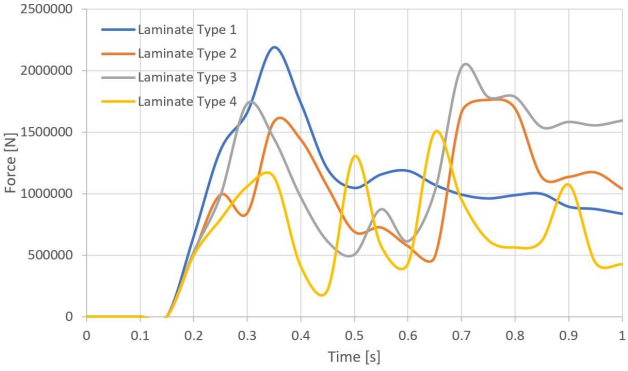

Figure 35: Force – Time of each type of laminate based on the impact at a speed of 5 knots

as presented in Figures 35 and 36, which means the ship's bow was touching the pier. Moreover, even though type 1 showed a reverse movement as indicated in Figure 36, its contact force was not zero, and this means the bounce motion occurred while the ship's structure was still touching the pier. Meanwhile, no bounce motion was discovered in

the other types. The laminate type 4 was observed to have the furthest forward movement of 1.9 m compared to the other types. It can be said that type 4 is relatively slow in absorbing ship-pier collision energy.

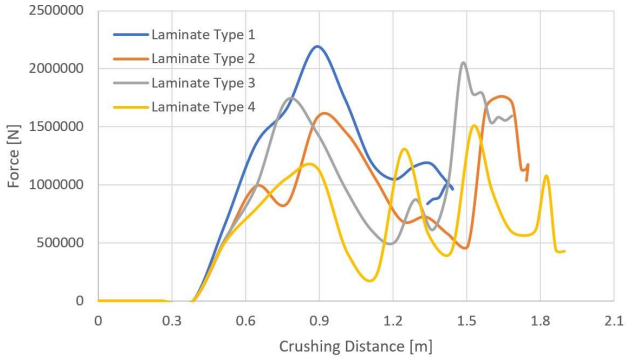

Figure 36: Force – displacement of each type of laminate based on the impact at a speed of 5 knots

Furthermore, the kinetic energy graph in Figure 37 shows that the ship's speed decreased with the kinetic energy moving close to zero as the simulation time ranged from 1 second, which is the duration for its completion. However, laminate type 4 has shown that the collision event is still running even though the simulation time was over,

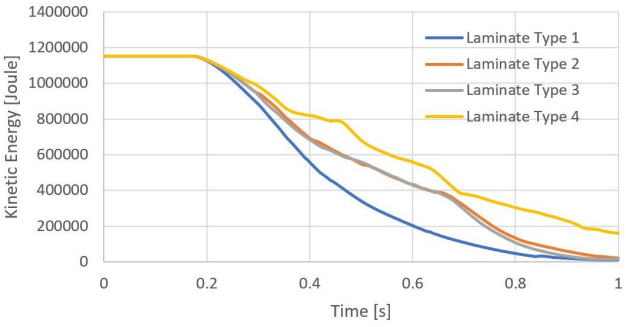

Figure 37: Kinetic Energy – Time of each type of laminate based on impact at a speed of 5 knots

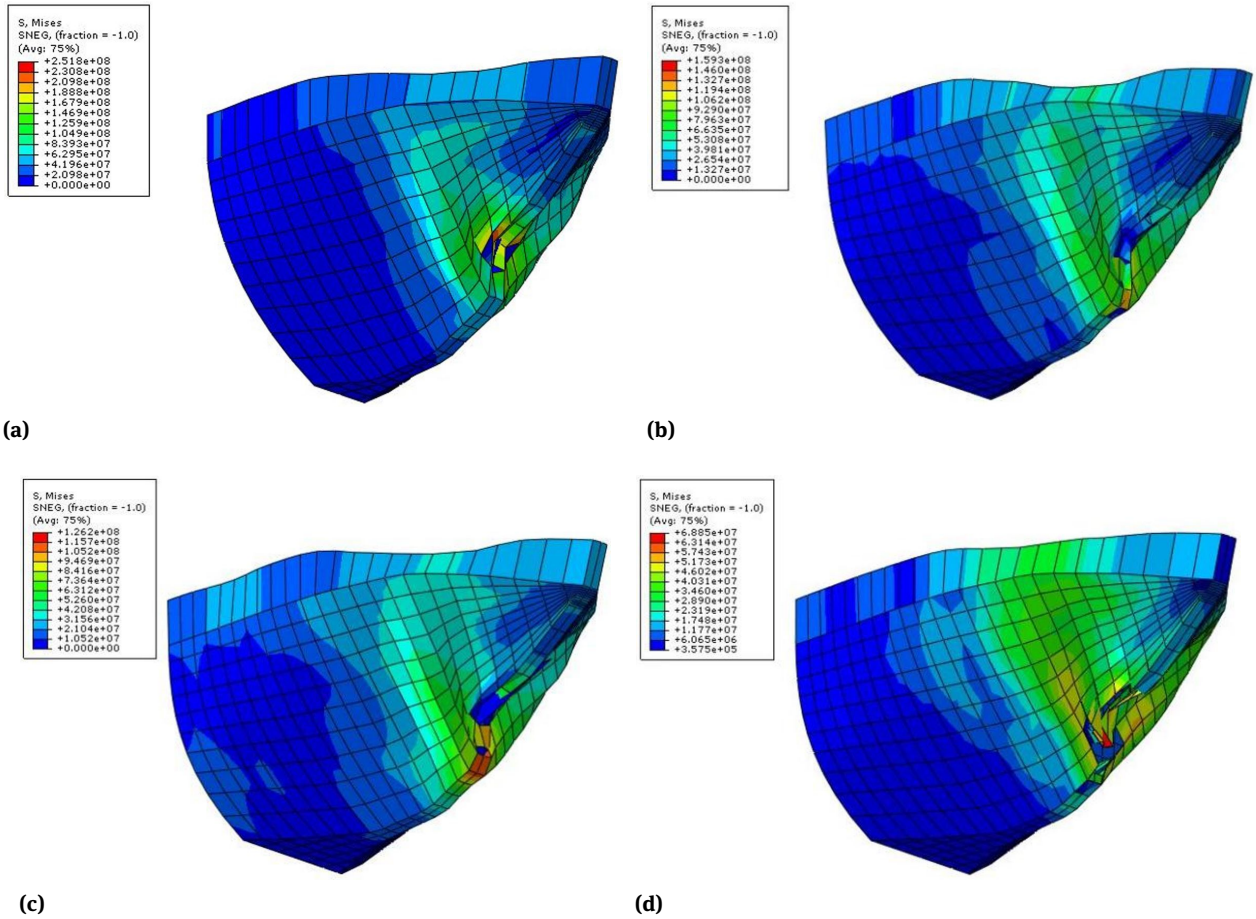

Figure 38: Deformation of hull construction due to impact at 5 knots: (a) Laminate type 1, (b) Laminate type 2, (c) Laminate type 3, (d) Laminate type 4

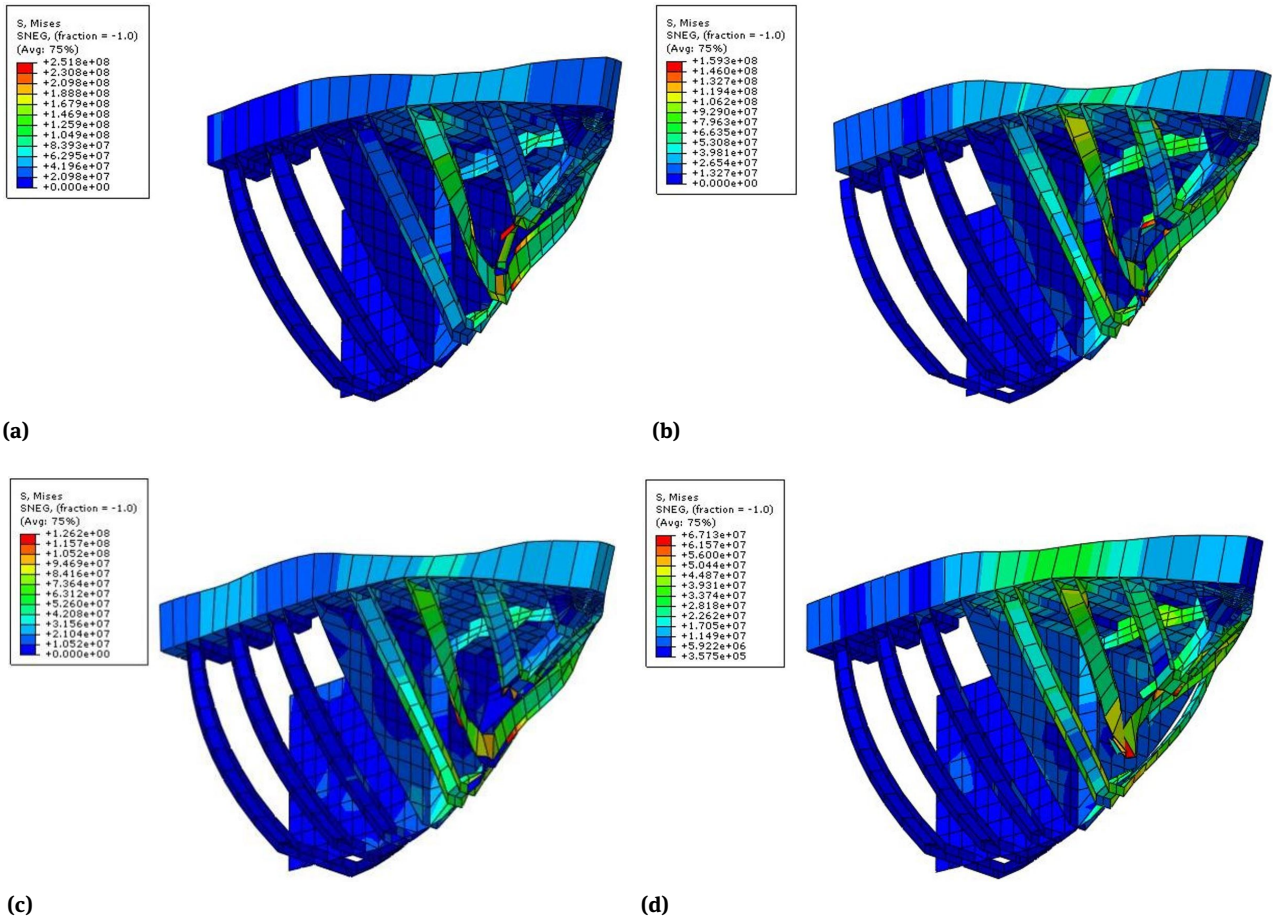

Figure 39: Deformation of bow construction due to impact at 5 knots: (a) Laminate type 1, (b) Laminate type 2, (c) Laminate type 3, (d) Laminate type 4

as observed in previous results. In contrast, the collision event was discovered to have ended in types 2 and 3 without any bounce. It means that the collision occurred with the hull position stopped and still stuck or attached to the pier.

The level of damage to the bow of each laminate type is presented in Figures 38 and 39, and all four types were found to have a higher level of damage at a speed of 5 knots compared to the previous lower speeds. The damage was discovered to have spread to the deck construction with significant deformation of the deck and bulwark, Figure 38. Moreover, the deformation in the stem frame and stem bar also appears to be larger, but the increase in the damage did not change the condition of global ship safety with the ship collision bulkheads observed to be intact without any tear, and this means the ship is still afloat and safe.

The simulation model at different collision speeds and types of laminations showed that the HCGFRP could be used as a hull material. It is observed from the possibility of increasing the thickness of the laminate (number of layers) to increase the safety factor of the ship under static loading. Meanwhile, It does not apply under dynamic loading such that the addition of the number of layers did not improve the ability of the ship to reduce the impact load. However, the damping of the impact force was indicated by the material's stiffness that was represented as the modulus of elasticity. The type 1 laminate, which has the largest modulus of elasticity, was discovered to have the ability to reduce the kinetic energy of collisions faster than the others. It means that a higher level of construction rigidity can reduce the collision energy more quickly. However, the rapid absorption of the collision energy also can cause an increase in the motion acceleration response. The significant acceleration response might negatively impact the passengers or crew, primarily when the collision occurs at a very high speed. However, it is important to note that this acceleration is not an essential consideration in the case of

this ship-pier collision because the process usually occurs at a relatively slow speed below 5 knots.

An increment in the layer thickness or number was able to reduce the stress in the collision as indicated in types 3 and 4 that have smaller maximum stress than 1 and 2. Meanwhile, it does not affect the failure, especially in element deletion animation, which is usually determined based on the maximum fracture strain. It means that the element deletion needs to be simulated when the element is deformed beyond the maximum fracture strain limit, even though the effective von Mises stress is much smaller than the other models. It was observed that type 1 reached a von Mises stress of 251 MPa, Figure 39a, but it has smaller damage than type 4, which only had 67.1 MPa as presented in Figure 39d. Moreover, the construction is also declared failed when it exceeds the maximum tensile strength limit. It is also important to note that this controversy associated with the determination of the failure criteria does not affect the suitability of the HCGFRP material as a hull material because the collision bulkhead remains intact in all types of the laminated HCGFRP material, and each collision velocity condition was between 3-5 knots.

6 Conclusion

Collision analysis was conducted to identify the level of damage experienced by the ship's bow structure, focusing on the damage to cause a leak that can lead the ship capsizing. The damage to the bow structure on the collision event at 3 knots was deformed, and fractures of stem structures. It was found that the collision damage could not cause the hull leakage. Meanwhile, tear damage was found in the bow structure on the collision event at 4 knots. This condition can allow the entry of water into the forepeak tank. In comparison, the damage at 5 knots was discovered to spread and be significantly occurred at the deck and bulwark structures. The more extensive deformation can also be found on the stem frame and bar. However, the increase in the level of damage did not change the condition of global ship safety because the water was observed only flooding the forepeak tank while the collision bulkhead was still intact and there were no tears.

The simulation conducted at different speeds of the collision and types of laminations showed the collision bulkhead was intact for all types of laminated HCGFRP material. Therefore it can be concluded that HCGFRP can be adopted as a surrogate hull material.

Acknowledgement: The authors appreciate the Department of Naval Architecture Engineering, Faculty Diponegoro University, which facilitated the mechanical testing experiment of the hybrid coir-glass fiber reinforced polyester polymer composite.

Funding information: The authors state no funding involved.

Author contributions: All authors have accepted responsibility for the entire content of this manuscript and approved its submission.

Conflict of interest: The authors state no conflict of interest.

References

[1] Sen T, Reddy HJ. Application of sisal, bamboo, coir, and jute natural composites in structural up-gradation. Int J Innov Manag Technol. 2011;2(3):186–91.

[2] Shenoi RA, Dulieu-Barton JM, Quinn S, Blake JI, Boyd SW. Composite materials for marine applications: key challenges for the future. In: Nicolais L, Meo M, Mileilla M, editors. Composite Materials. London: Springer; 2011. p. 69–89.

[3] Mochane MJ, Mokhena TC, Mokhothu TH, Mtibe A, Sadiku ER, Ray SS, et al. Recent progress on natural fiber hybrid composites for advanced applications: A review. Express Polym Lett. 2019;13(2):159–98.

[4] Tsampas SA, Greenhalgh ES, Ankersen J, Curtis PT. Compressive failure of hybrid multidirectional fibre-reinforced composites. Compos, Part A Appl Sci Manuf. 2015;71:40–58.

[5] Aisyah HA, Paridah MT, Khalina A, Sapuan SM, Wahab MS, Berkalp OB, et al. Effects of fabric counts and weave designs on the properties of Laminated Woven Kenaf/Carbon fibre reinforced epoxy hybrid composites. Polymers (Basel). 2018 Nov;10(12):1320.

[6] Nisini E, Santulli C, Liverani A. Mechanical and impact characterization of hybrid composite laminates with carbon, basalt and flax fibres. Compos, Part B Eng. 2017;127:92–9.

[7] Ralph C, Lemoine P, Archer E, McIlhagger A. Mechanical properties of short basalt fibre reinforced polypropylene and the effect of fibre sizing on adhesion. Compos, Part B Eng. 2019;176:107260.

[8] Flynn J, Amiri A, Ulven C. Hybridized carbon and flax fiber composites for tailored performance. Mater Des. 2016;102:21–9.

[9] Sapuan SM, Aulia HS, Ilyas RA, Atiqah A, Dele-Afolabi TT, Nurazzi MN, et al. Mechanical Properties of Longitudinal Basalt/Woven-Glass-Fiber-reinforced Unsaturated Polyester-Resin Hybrid Composites. Polymers (Basel). 2020 Sep;12(10):2211.

[10] Vinayagamoorthy R, Rajeswari N. Mechanical performance studies on Vetiveria zizanioides/jute/glass fiber-reinforced hybrid polymeric composites. J Reinf Plast Compos. 2014;33(1):81–92.

[11] Jothibasu S, Mohanamurugan S, Vijay R, Singaravelu DL, Vinod A, Sanjay M. Investigation on the mechanical behavior of areca

sheath fibers/jute fibers/glass fabrics reinforced hybrid composite for light weight applications. J Ind Text. 2018;49(8):1036–60.
[12] Aslan M, Tufan M, Küçükömeroglu T. Tribological and mechanical performance of sisal-filled waste carbon and glass fibre hybrid composites. Compos, Part B Eng. 2018;140:241–9.
[13] Rao HR, Rajulu AV, Reddy GR, Reddy KH. Flexural and Compressive Properties of Bamboo and Glass Fiber-reinforced Epoxy Hybrid Composites. J Reinf Plast Compos. 2009;29(10):1446–50.
[14] Retnam BS, Sivapragash M, Pradeep P. Effects of fibre orientation on mechanical properties of hybrid bamboo/glass fibre polymer composites. Bull Mater Sci. 2014;37(5):1059–64.
[15] Arif MF, Kumar S, Shah T. Tunable morphology and its influence on electrical, thermal and mechanical properties of carbon nanostructure-buckypaper. Mater Des. 2016;101:236–44.
[16] Nurazzi NM, Khalina A, Sapuan SM, Rahmah M. Development of sugar palm yarn/glass fibre reinforced unsaturated polyester hybrid composites. Mater Res Express. 2018;5(4):045308.
[17] Prajapati P, Sharma C, Shrivastava R, Rana RS. Evaluation of mechanical properties of coir and glass fiber hybrid composites. Mater Today Proc. 2018;5(9):19056–62.
[18] Islam MR, Gupta A, Rivai M, Beg MD. Characterization of microwave-treated oil palm empty fruit bunch/glass fibre/polypropylene composites. J Thermoplast Compos Mater. 2017;30(7):986–1002.
[19] Nourbakhsh A, Ashori A, Kargarfard A. Evaluation of multiwalled carbon nanotubes as reinforcement for natural fiber-based composites. Polym Compos. 2016;37(11):3269–74.
[20] Asyraf MR, Ishak MR, Sapuan SM, Yidris N. Comparison of Static and Long-term Creep Behaviors between Balau Wood and Glass Fiber Reinforced Polymer Composite for Cross-arm Application. Fibers Polym. 2021;22(3):793–803.
[21] Asyraf MR, Ishak MR, Sapuan SM, Yidris N. Influence of Additional Bracing Arms as Reinforcement Members in Wooden Timber Cross-Arms on Their Long-Term Creep Responses and Properties. Appl Sci (Basel). 2021;11(5):2061.
[22] Asyraf MR, Ishak MR, Sapuan SM, Yidris N, Ilyas RA. Woods and composites cantilever beam: A comprehensive review of experimental and numerical creep methodologies. J Mater Res Technol. 2020;9(3):6759–76.
[23] Fiore V, Scalici T, Sarasini F, Tirilló J, Calabrese L. Salt-fog spray aging of jute-basalt reinforced hybrid structures: flexural and low velocity impact response. Compos, Part B Eng. 2017;116:99–112.
[24] Bodur MS, Englund K, Bakkal M. Water absorption behavior and kinetics of glass fiber/waste cotton fabric hybrid composites. J Appl Polym Sci. 2017;134(47):45506.
[25] Misri S, Leman Z, Sapuan SM, Ishak MR. Mechanical properties and fabrication of small boat using woven glass/sugar palm fibres reinforced unsaturated polyester hybrid composite. IOP Conf Ser Mater Sci Eng. 2010;11:012015. https://doi.org/10.1088/1757-899X/11/1/012015.
[26] Renjith R, Nair RP. Structural analysis of NFRP composite boat hull using finite element method. J Offshore Struct and Tech. 2019;6(1):10–7.
[27] Tikupadang K, Palungan MB, Buku A, Manuhutu H. The utilization of agave cantula roxb as composite strength on fishing boat hull. IOP Conf Ser Mater Sci Eng. 2021;1088(1):012101. https://doi.org/10.1088/1757-899X/1088/1/012101.
[28] Jones RM. Mechanics of composite materials. 2nd ed. London: Taylor & Francis; 1999.
[29] Taury HA, Zakki AF. Normal Mode Analysis of Traditional Purse Seine in Central Java Indonesia. Kapal: J Mar Sci Technol. 2018;15(1):33–7.